Electrochemical Construction of Novel C_{60} Derivative/PPV Composite Adlayer on Cu(111) and Their Current/Voltage Characteristics

Mei-Juan Han,† Li-Jun Wan,* Sheng-Bin Lei, Hong-Mei Li, Xiao-Lin Fan, Chun-Li Bai,* Yu-Liang Li, and Dao-Ben Zhu

Institute of Chemistry, Chinese Academy of Sciences, Beijing 100080 China

Received: June 11, 2003; In Final Form: October 5, 2003

Composite adlayer of novel C_{60} derivative and BH−PPV was constructed on Cu(111) electrode surfaces in solution. First, hexa(sulfobutyl)C_{60} and BH−PPV adlayers were prepared, respectively. Then, adding another molecule resulted in the formation of a composite adlayer, demonstrated by cyclic voltammetry, UV−visible spectra, and in situ STM. All of these molecules form well-ordered adlayers. Their molecular features clearly appeared in high-resolution STM images. The electronic properties of these molecular adlayers were studied by using a capillary tunnel junction method. The $I-V$ characteristics show different nonlinear behavior for the three adlayers. The present results provide a concrete example of the systematic design of self-organized layers with promising properties and demonstrate that controllable layer by layer composite film can be constructed at liquid/solid interface at room temperature.

Introduction

Recently, there is an increasing interest in the fabricating of composite and multilayer nanostructures with electrostatic interactions.[1−4] The fabrication of composite and multilayer structures is an important approach to improve performance and function of materials. The coadsorption of functional molecules on metal surface under potential control is a facile and powerful method to fabricate controllable nanoscale film materials that possess promising properties. The adsorption behavior of charge-transfer complexes on Cu(111) surface has been investigated successfully,[5] which encourages us to further explore the coadsorption of organic functional molecules. In this work, we aim mainly to study the new structure and electronic properties of novel C_{60} derivative and BH−PPV (poly{(2,5-bis(3-bromo trimethylammonio propoxy)-phenylene-1,4-divinylene)-*alt*-1,4-(2,5-bis (2-(2-hydroxylethoxy) ethoxy)) phenylenevinylene}) bimolecular composite adlayer constructed by electrostatic interactions in 0.1 M $HClO_4$ solution.

The wide range of physical and chemical properties of fullerenes makes them promising candidates for superconductors, photoconductors, semiconductors, ferromagnets, and optical materials.[6−10] One of the important issues in fullerene studies is its adsorption and ordering on various substrates. Up to now, various techniques have been applied in this field. Scanning tunneling microscopy (STM) has proven to be an important tool for the study of the interaction of fullerenes with both metal and semiconductor substrates. The adsorption geometry, phase transition, and chemical reactivity have all been well investigated by STM. C_{60} can adsorb on various substrates such as Au,[11,12] Ag,[13−15] Al,[16] Cu,[17,18] Si,[19,20] and GaAs[11] and form well-ordered adlayers on them under UHV (ultrahigh vacuum) or in solution.[21−24] Among these substrates, the Cu(111) surface is one of the most ideal surfaces for the growth of C_{60} film with a structure similar to the bulk,[25] since the lattice mismatch is small (2%) between the nearest neighbor distance (1.0 nm) of the bulk C_{60} crystal and 4 times of the Cu−Cu nearest neighbor distance (1.02 nm). The study of C_{60} adsorption on Cu(111), (110), and (100) surfaces with X-ray photoelectron spectroscopy (XPS), high-resolution electron energy loss spectroscopy (HREELS), and other techniques[26] showed that the Cu substrate donates charge to the lowest unoccupied molecular orbital (LUMO) of C_{60}. So, the C_{60} molecules can form a stable adlayer on Cu surface, even at room temperature.

In this paper, we report the results of electrochemical construction of composite adlayer of hexa(sulfobutyl)C_{60} (abbr., HSC_{60}) and BH−PPV on Cu(111). Although many physical methods, such as MBE (molecular beam epitaxy) and LB (Langmuir−Blodgett), have been well used to prepare controllable thin films layer by layer, the electrochemical technique is another important approach to construct two- and three-dimensional structures. Scheme 1 shows the chemical structures of HSC_{60} and BH−PPV molecules. The incorporation of sulfobutyl chains with C_{60} cage improves the solubility and processability. PPV and its derivatives belong to one of the most extensively investigated conjugated polymers which can be used for fabricating batteries, sensors, and electrochromic devices as well as efficient and long-living electroluminescent devices.[27−29] The use of conjugated polymers in devices has several advantages such as ease of fabrication and low cost. In addition, the fabrication of multilayer structure can be used to improve device performance or obtaining higher device functionality, by combining two or more desirable properties. The composite adlayer prepared by PPV and C_{60} may produce interesting electronic and electroluminescent property for the use of nanoscale devices. Because of the promising properties of PPV and C_{60}, many groups have been studying the applications of these materials. For example, H. Mattoussi et al.[30] demonstrated that a heterostructure device made of PPV and C_{60} have the rectifying photovoltaic function. High rectification ratios and large photoresponses were reported for MEH−PPV/C_{60} heterostructure devices.[27] According to the reported results,[30,31] the heterojunc-

* Corresponding authors. Tel. and fax: +86-10-62558934; e-mail: wanlijun@iccas.ac.cn.

† Also in Graduate School of Chinese Academy of Sciences, Beijing, China.

10.1021/jp035659g CCC: $27.50
Published on Web 12/11/2003

SCHEME 1: Chemical Structures of (a) Hexa(sulfobutyl)C_{60} ($C_{84}H_{48}O_{18}S_6Na_6$), (b) BH−PPV ($C_{36}H_{56}O_8N_2Br_2$)

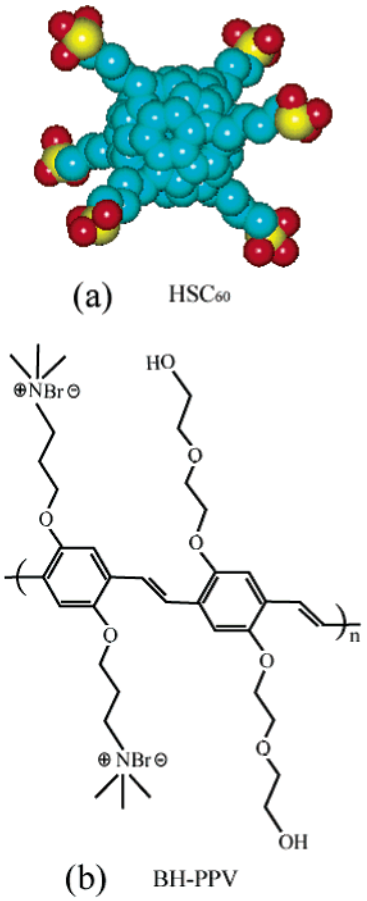

tion devices made of PPV and C_{60} have the potential for use as sensitive solar cells with low dark currents and high open circuit voltages. That is to say, by changing a component in the layer, various materials with novel electronic and optical properties could be obtained.

In the present study, the bimolecular adlayer with enhanced electronic properties has been demonstrated. In situ STM imaging revealed the structures of HSC_{60}, BH−PPV, and HSC_{60}/BH−PPV layers. According to the orientation of molecular rows and the intermolecular distance, unit cells of these molecules were determined and the structural models were proposed for the three layers. In current/voltage ($I-V$) curve of the HSC_{60}/BH−PPV composite monolayer, the rectification region is extended to a wider potential region than that in the single component monolayer of either HSC_{60} or BH−PPV. The composite monolayer film should be a promising material for preparing nanoscale electronic device.

Experimental Section

A bulk Cu(111) single-crystal disk with a diameter of 10 mm (MaTeck, Germany) was used as a working electrode for both electrochemical measurements and in situ STM observation. The details of the sample preparation were described elsewhere.[32,33] Briefly, after having been mechanically polished with diamond paste successively down to 0.05 μm in particle diameter, the sample was further treated by electropolishing in a phosphoric acid solution (50 mL of 85% H_3PO_4 and 50 mL water) at 0.8−1.0 A cm^{-2} for 3−5 s. The Cu crystal was then rinsed repeatedly with ultrapure water (Millipore-Q).

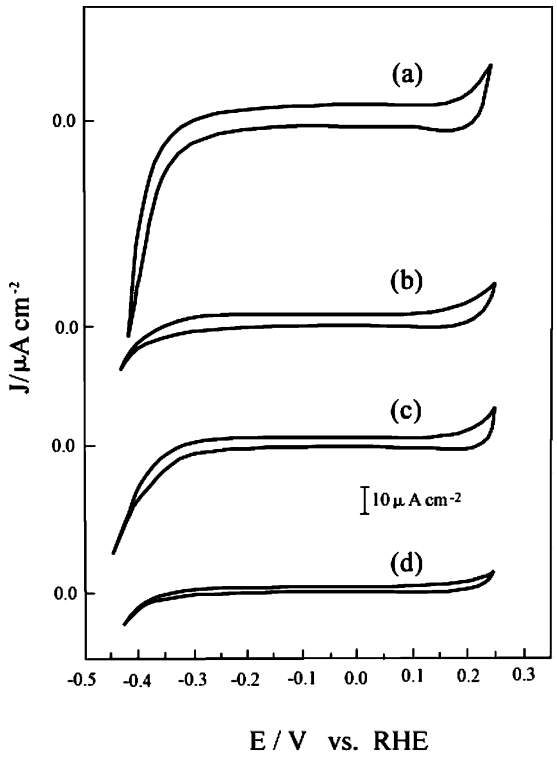

Figure 1. Cyclic voltammograms of Cu(111) in (a) 0.1 M $HClO_4$, (b) 0.1 M $HClO_4$ + 1 mM HSC_{60}, (c) 0.1 M $HClO_4$ + 1 mM BH−PPV, and (d) 0.1 M $HClO_4$ + 1 mM HSC_{60} + 1mM BH−PPV. The potential scan rate was 50 mV s^{-1}.

The in situ STM apparatus was a Nanoscope E (Digital Instrument Inc., Santa Barbara, CA). Tunneling tips were prepared by electrochemical etching of a tungsten wire (0.25 mm in diameter) in 0.6 M KOH. 12−15 V AC was applied until the etching process stopped. The W tips were then coated with a clear nail polish to minimize the faradaic current. The STM images shown here were acquired in the constant-current mode to evaluate corrugation heights of adsorbed molecules. All electrolyte solutions were prepared by diluting ultrapure $HClO_4$. A homemade electrochemical cell contains a reversible hydrogen electrode (RHE) in 0.1 M $HClO_4$ as a reference electrode and a Pt counter electrode. All electrode potentials were reported with respect to RHE. HSC_{60} and BH−PPV were prepared by the method described in the literature.[34,35]

The $I-V$ characteristics were measured using the capillary tunnel junction method, which was described in detail in the reference.[36]

The UV−visible adsorption spectra were recorded on a UV-1601 spectrophotometer (Shimadzu) in solution.

Results and Discussion

Cyclic Voltammetry. Because the preparation of the monolayer was carried out in solution, it is necessary to understand the electrochemical behavior. The Cu(111) electrode was initially examined by cyclic voltammetry in 0.1 M $HClO_4$ in the absence of organic molecules for comparison with former results,[32,33] as shown in Figure 1a. After the examination, the sample was transferred into a 0.1 M $HClO_4$ solution containing 1 mM of the organic molecules. The cyclic voltammograms (CVs) at Cu(111) for HSC_{60}, BH−PPV and composite adlayers were measured. There is no obvious feature in the CVs in solutions containing these molecules. Figure 1b and c are CVs of Cu(111) in 0.1 M $HClO_4$ in the presence of 1 mM HSC_{60} and BH−PPV, respectively. It is obvious that the double-layer

region extends over a wide potential region. The overall shape of the CVs is similar to that of the bare Cu(111) obtained in 0.1 M $HClO_4$, indicating that no electrochemical reaction took place at least in the double-layer potential region.[32,33] Only the electric charge involved in the double-layer potential range becomes smaller because of the adsorption of HSC_{60} and BH−PPV molecules. Figure 1d shows a CV of Cu(111) in 0.1 M $HClO_4$ + 1 mM BH−PPV and HSC_{60}. The double-layer region is extended from −0.33 to 0.15 V. The electric charge involved in the double-layer potential range becomes much smaller compared with Figure 1b and c. These characteristics can be manifested from the nonfaradaic current density values of different adlayers. The nonfaradaic current density values of bare Cu, HSC_{60}, and BH−PPV adlayers are ca. 3.2, 1.72, and 1.45 $\mu A/cm^2$, while the density value of the composite adlayer is ca. 0.41 $\mu A/cm^2$.

The details of the adsorption structures of these three molecules were investigated by in situ STM.

In Situ STM. *(1) Hexa(sulfobutyl)C_{60} Adlayer.* The atomic image of the Cu(111)−(1 × 1) structure was routinely discerned on atomically flat Cu(111) terraces in the absence of the molecules in 0.1 M $HClO_4$ to determine the crystal orientation of the molecular adlayer with the underlying Cu(111) lattice.[32,33] After the atomic resolution image of Cu(111) was achieved, a small amount of HSC_{60} solution was directly injected into the cell to form a HSC_{60} adlayer. Figure 2a is an STM image of the HSC_{60} adlayer in 0.1 M $HClO_4$ + 1 mM HSC_{60}. This image was acquired at −0.2 V. According to previous results,[26] the interactions between C_{60} and the Cu(111) substrate are strong, and charge transfer takes place from the substrate to C_{60}. Therefore, C_{60} molecules can form ordered structure on the Cu(111) surface even at room temperature. There are almost no defects in Figure 2a. The molecular array is seen to extend over wide atomically flat terraces. The molecular rows cross at an angle of either 60° or 120° within an experimental error of ±2°. By comparison with the Cu(111)−(1 × 1) atomic image, it is found that all molecular rows are parallel to the ⟨110⟩ direction of underlying Cu(111) lattice. The intermolecular distances along the ⟨110⟩ orientation were measured to be 0.98 ± 0.02 nm, corresponding to 4 times the Cu(111) lattice distance. On the basis of the orientation of molecular rows and the intermolecular distance, we conclude that the observed HSC_{60} adlayer is in a (4 × 4) structure with a surface coverage of 0.0625. A unit cell is superimposed in Figure 2a. This structure is consistent with the results reported by other groups studying C_{60} adlayers on Cu(111) in UHV.[17,18]

STM images acquired with even higher resolution allowed us to determine the internal structure and orientation of each HSC_{60} molecule. Figure 2b is a high-resolution STM image of the HSC_{60} adlayer. There exists two single molecular defects in the image, indicated by arrows where the molecules are missing. The features of the molecules can be clearly seen. Clearly, each spot corresponding to a HSC_{60} molecule in the low-resolution image is now split into a set of three bright spots. They are believed to be the manifestation of the intramolecular structure of C_{60} cage. Such a configuration is consistent with C_{60} on Cu(111) and Si(111) in UHV by experiment and theoretical calculation.[17,18,37] It is clear from the observation that the C_{60} cage dominates the molecular orientation, resulting in a stable adlayer. Because of the abundant electronic states of the C_{60} core, the chains of the HSC_{60} cannot be observed clearly.

On the basis of these STM image features and previous results,[17,18,38] a structural model for HSC_{60} adlayer on the Cu(111) surface is tentatively proposed in Figure 2c. The

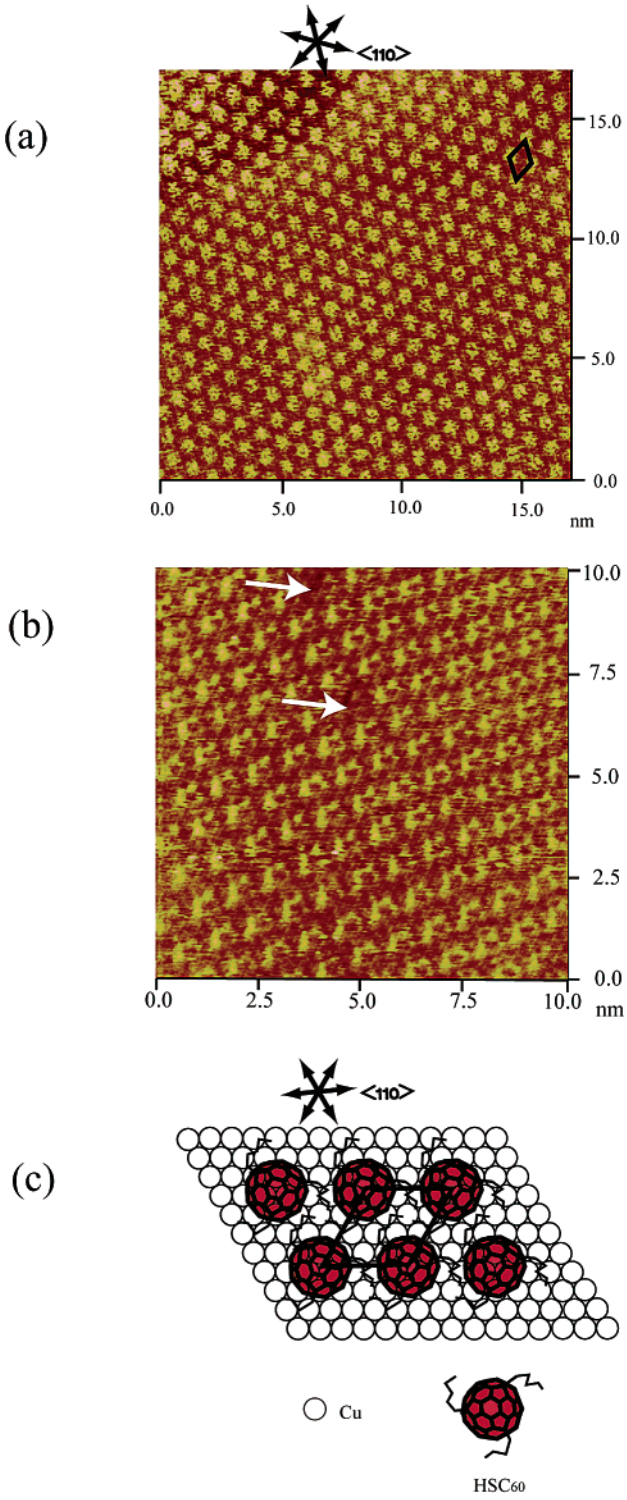

Figure 2. (a) Large-scale STM images of a Cu(111)−(4 × 4)−HSC_{60} adlattice acquired at −0.2 V. Tunneling current was 2 nA. Scanning rate was 15.26 Hz. (b) In situ STM image of HSC_{60} adlayer on Cu(111) in 0.1 M $HClO_4$. Tunneling current was 2 nA. Scanning rate was 20.35 Hz. (c) Proposed model of HSC_{60} adlayer on Cu(111) surface.

molecular center is placed on the three-fold hollow site of the substrate, the same coordination as that reported in the literature.[17,18] The three pentagonal rings surrounding one hexagonal ring of a C_{60} molecule are located on bridge sites. The side chains in C_{60} cage face down on the Cu(111) surface. In this model, there is a maximum coordination of C_{60} molecule to Cu(111) substrate, resulting in a stable adlayer. The ordered

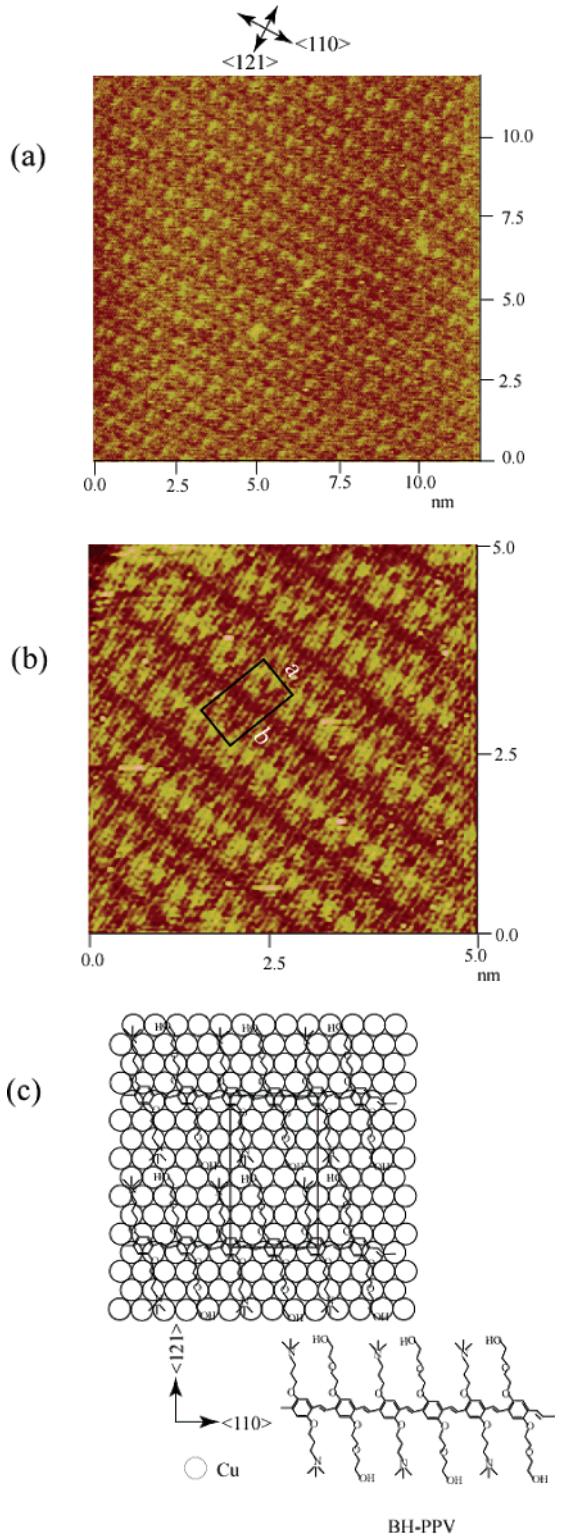

Figure 3. (a) STM image of BH−PPV molecules on Cu(111) in 0.1 M $HClO_4$ containing 1 mM BH−PPV at −0.2 V. Tunneling current was 2 nA. Scanning rate was 15.26 Hz. (b) Higher resolution STM image of BH−PPV array on Cu(111) in 0.1 M $HClO_4$. Tunneling current was 2 nA. Scanning rate was 20.35 Hz. (c) Schematic representation for the $(4 \times 4\sqrt{3})$ structure.

(4×4) structure was consistently observed in the double-layer potential region from −0.30 to 0.1 V.

(2) BH−PPV Adlayer. BH−PPV molecule becomes a positively charged ion in solution. The image shown in Figure 3a is a typical STM image for the ordered BH−PPV adlayer formed on the Cu(111) surface. The image was acquired at −0.2 V in 0.1 M $HClO_4$ solution containing 1 mM BH−PPV. The STM image in Figure 3b shows more details of the packing arrangement and the internal structure of the BH−PPV adlayer. The two main spots along with side chains form a rectangle unit. The bright spots along with side chains in STM images are attributed to two benzene rings of a BH−PPV unit. The molecules form an ordered two-dimensional network. The width of each rectangle along direction *a* is ca. 1.0 ± 0.05 nm, and the length of the molecule along direction *b* is 1.8 ± 0.05 nm, consistent with the results optimized by HyperChem. The angle between the two directions is 90° within an experimental error of ±2°. A unit cell for the molecular adlayer is outlined in Figure 3b. According to the intermolecular distance and orientation of molecular rows, the adlayer can be defined as a $(4 \times 4\sqrt{3})$ structure with a surface coverage of 0.0313. Figure 3c shows a proposed schematic representation of BH−PPV on Cu(111) surface. We tentatively proposed that the two benzene rings of the BH−PPV occupy the three-fold hollow sites.

(3) HSC_{60} and BH−PPV Adlayer. The alternating adsorption of oppositely charged adsorbates is a facile and powerful method to fabricate controllable layer by layer nanoscale films. The composite monolayer was prepared on Cu electrode surface by alternating adsorption of oppositely charged HSC_{60} and BH−PPV. Briefly, a well-defined BH−PPV layer was first prepared on Cu(111) surface. Then, a HSC_{60} solution was added over the BH−PPV layer. The experiments in opposite order were also done, and the STM images were similar. Owing to their opposite charges, a composite monolayer of HSC_{60}/BH−PPV was automatically formed. Figure 4a is a typical STM image of the composite adlayer on Cu(111) in 0.1 M $HClO_4$. The appearance of the adlayer is completely different from that in Figure 2 and Figure 3, although the STM imaging conditions here are almost the same as those used in recording the other adlayers. A two-dimensional network with four-fold symmetry can be seen in the image. To prove the formation of a composite adlayer, UV−vis spectroscopy was used to investigate the behaviors of these molecules. Figure 4b shows the absorption spectrum of BH−PPV, HSC_{60}, and the composite molecules in solution. A slight blue-shift of the absorbance maximum can be seen in the spectrum compared to the spectra of BH−PPV at 443 nm. The blue-shift of the absorbance maximum is the result of the coadsorption of BH−PPV and HSC_{60}, indicating the formation of a composite adlayer. The formation of a well-defined adlayer is dependent on the chemical structure of molecules and the interactions among molecules as well as molecule and substrate. In the present study, it can be seen from the molecular structures of Scheme 1 that the two molecules are positively and negatively charged. HSC_{60} is negatively charged, while BH−PPV is positively charged. Owing to the static attraction, the side chains in the two kinds of molecules should be linked together by an electrostatic reaction, resulting in a composite adlayer. According to intermolecular distance and the orientation of the molecular rows to the underlying Cu(111) lattice, the composite adlayer has a $(4 \times 3\sqrt{3})$ structure. This arrangement is a more densely packed phase than both of the single component adlayers. A unit cell is outlined in Figure 4a. The bright spots in the STM image are assumed from C_{60} cages from the chemical structure difference in the two molecules. A tentative model for the composite adlayer on Cu(111) is proposed in Figure 4c.

I−V Features. The experiments reveal a novel *I*−*V* feature in the composite monolayer with high stability and reproducibility. Figure 5 presents typical current−voltage (*I*−*V*) curves of the three types of adlayers measured by the method of

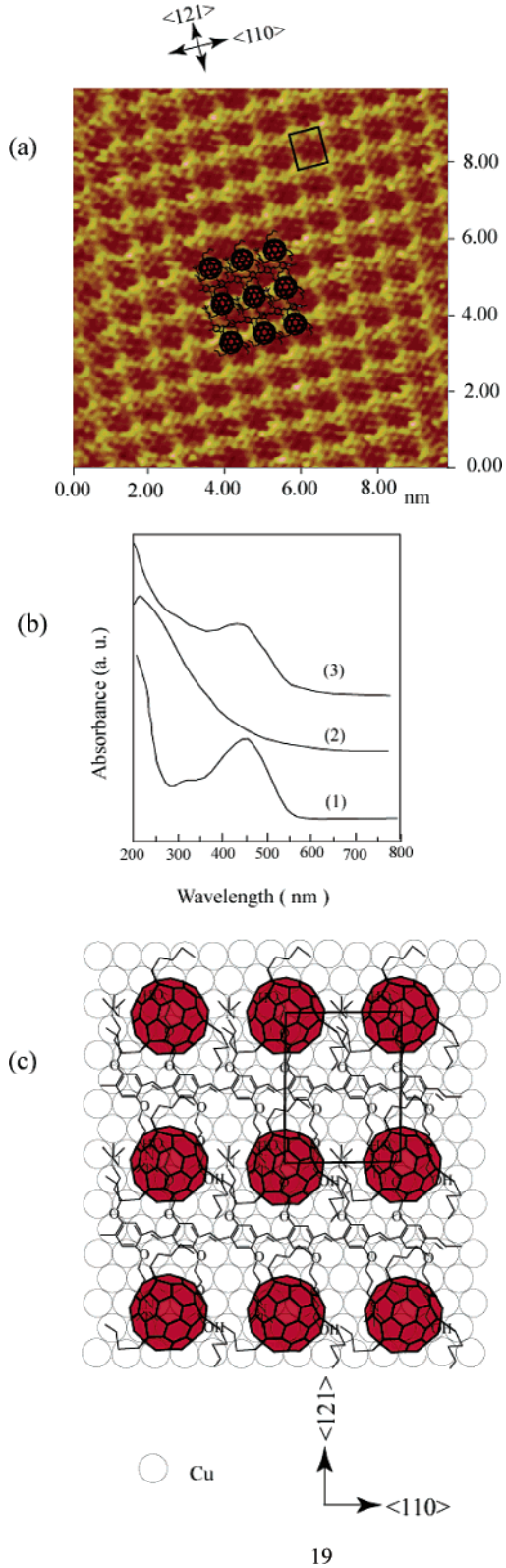

19

Figure 4. (a) Higher resolution STM image of the composite adlayer of HSC_{60} and BH−PPV on Cu(111) in 0.1 M $HClO_4$. Tunneling current was 2 nA. Scanning rate was 20.35 Hz. (b) UV−vis absorption spectrum of (1) BH−PPV, (2) HSC_{60}, and (3) BH−PPV and HSC_{60}. (c) Structural model for the composite adlayer on Cu(111).

capillary tunnel junction.[36] In this experiment, the molecules were self-assembled on a copper surface. A tunnel junction was formed inside a capillary. The details of the technique are described in the literature.[36] Repeated measurements of inde-

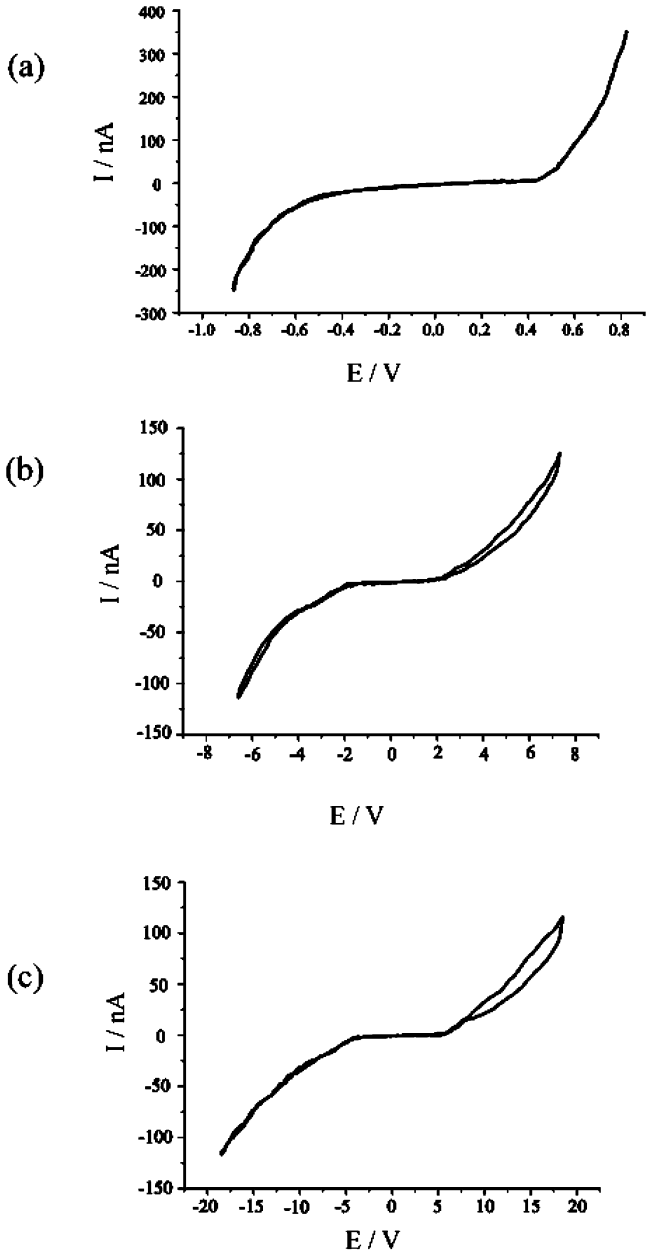

Figure 5. The current−voltage characteristics of the adlayers of (a) HSC_{60}, (b) BH−PPV, and (c) HSC_{60} and BH−PPV.

pendently prepared junctions have produced reliable and reproducible results. From Figure 5, nonlinear characteristics have been observed in all junctions of the three types of molecular film. The tunneling between the substrate and molecular layer is generally a function of the electronic state of molecules. The asymmetric current−voltage characteristics of these molecules suggest that they have a potential application in nanoscale electronic device such as rectifier. As shown in Figure 5, rectified behavior was clearly observed for these adlayers. The rectified region of HSC_{60} in Figure 5a is extended from −0.5 to 0.5 V consistent with that of C_{60}, BH−PPV from −2 to 2 V in Figure 5b. However, the rectified region of the composite monolayer in Figure 5c is extended from −5 to 5 V broader than that of in Figure 5a and 5b. This result is likely due to the interaction between the HSC_{60} and BH−PPV molecules. The interactions enhance the potential barrier of the composite adlayer and the energy gap broadened from −5 to 5 V.

Conclusion

The present results demonstrate for the first time that a well-ordered composite adlayer of HSC_{60} and BH−PPV can be prepared on Cu(111) in solution by electrostatic interactions between the two molecules. HSC_{60} and BH−PPV molecules form well-defined structures with (4×4) and $(4 \times 4\sqrt{3})$ symmetry, respectively. The composite adlayer has a different structure of $(4 \times 3\sqrt{3})$. The structural details of these adlayers are clearly revealed in high-resolution STM images. Structural models are tentatively proposed. Novel current/voltage characteristics are found in the composite adlayer. The rectified region extends from −5 to 5 V. The results indicated that the current/voltage characteristics could be controlled by changing component in the monolayer. The present results demonstrate that controllable layer by layer nanoscale composite film can be constructed at liquid/solid interface by electrochemical method that should be important in constructing electronic device.

Acknowledgment. Financial supports from National Natural Science Foundation of China (Nos. 20025308, 20177025, and 20203019), National Key Project on Basic Research (Grant G2000077501), and the Chinese Academy of Sciences are gratefully acknowledged.

References and Notes

(1) Khopade, A. J.; Caruso, F. *Biomacromolecules* **2002**, *3*, 1154.
(2) Krass, H.; Papastavrou, G.; Kurth, D. G. *Chem. Mater.* **2003**, *15*, 196.
(3) Cabibil, H. L.; Pham, V.; Lozano, J.; Celio, H.; Winter, R. M.; White, J. M. *Langmuir* **2000**, *16*, 10471.
(4) Zamlynny, V.; Zawisza, I.; Lipkowski, J. *Langmuir* **2003**, *19*, 132.
(5) Xu, Q.-M.; Zhang, B.; Wan, L.-J.; Wang, C.; Bai, C.-L.; Zhu, D.-B. *Surf. Sci.* **2002**, *517*, 52.
(6) Hebard; A. F.; Rosseinsky, M. J.; Haddon, R. C.; Murphy, D. W.; Glarum, S. H.; Palstra, T. T. M.; Ramirez, A. P.; Kortan, A. R. *Nature* **1991**, *350*, 600.
(7) Tanigaki, K.; Ebbesen, T. W.; Saito, S.; Mizuki, J.; Tsai, J. S.; Kubo, Y.; Kuroshima, S. *Nature* **1991**, *352*, 222.
(8) Allemand, P. M.; Khemani, K. C.; Koch, A.; Wudl, F.; Holczer, K.; Donovan, S.; Grüner, G.; Thompson, J. D. *Science* **1991**, *253*, 301.
(9) Imahori, H.; Sakata, Y. *Adv. Mater.* **1997**, *9*, 537.
(10) Janda, P.; Krieg, T.; Dunsch, L. *Adv. Mater.* **1998**, *10*, 1434.
(11) Sakurai, T.; Wang, X.-D.; Xue, Q. K.; Hasegawa, Y.; Hashizume, T.; Shinohara, H. *Prog. Surf. Sci.* **1996**, *51*, 263.
(12) Altman, E. I.; Colton, R. J. *Phys. Rev.* **1993**, *B48*, 18244.
(13) Giudice, E.; Magnano, E.; Rusponi, S.; Boragno, C.; Valbusa, U. *Surf. Sci.* **1998**, *405*, L561.
(14) Costantini, G.; Rusponi, S.; Giudice, E.; Boragno, C.; Valbusa, U. *Carbon* **1999**, *37*, 727.
(15) Butcher, M. J.; Nolan, J. N.; Hunt, M. R. C.; Beton, P. H.; Dunsch, L.; Kuran, P.; Georgi, P.; Dennis, T. J. S. *Phys. Rev.* **2001**, *B64*, 195401.
(16) Johansson, M. K. J.; Maxwell, A. J.; Gray, S. M.; Brühwiler, P. A.; Mancini, D. C.; Johansson, L. S. O.; Mårtensson, N. *Phys. Rev.* **1996**, *B54*, 13472.
(17) Hashizume, T.; Motai, K.; Wang, X. D.; Shinohara, H.; Saito, Y.; Maruyama, Y.; Ohno, K.; Kawazoe, Y.; Nishina, Y.; Pickering, H. W.; Kuk, Y.; Sakurai, T. *Phys. Rev. Lett.* **1993**, *71*, 2959.
(18) Maruyama, Y.; Ohno, K.; Kawazoe, Y. *Phys. Rev.* **1995**, *B52*, 2070.
(19) Ma, Y.-R.; Moriarty, P.; Upward, M. D.; Beton, P. H. *Surf. Sci.* **1998**, *397*, 421.
(20) Stimpel, T.; Schraufstetter, M.; Baumgärtner, H.; Eisele, I. *Mater. Sci. Eng.* **2002**, *B89*, 394.
(21) Yoshimoto, S.; Narita, R.; Tsutsumi, E.; Matsumoto, M.; Itaya, K.; Ito, O.; Fujiwara, K.; Murata, Y.; Komatsu, K. *Langmuir* **2002**, *18*, 8518.
(22) Zhang, Y.; Cao, X.; Weaver, M. J. *J. Phys. Chem.* **1992**, *96*, 510.
(23) Uemura, S.; Ohira, A.; Ishizaki, T.; Sakata, M.; Kunitake, M.; Taniguchi, I.; Hirayama, C. *Chem. Lett.* **1999**, 535.
(24) Uemura, S.; Sakata, M.; Taniguchi, I.; Kunitake, M.; Hirayama, C. *Langmuir* **2001**, *17*, 5.
(25) Motai, K.; Hashizume, T.; Shinohara, H.; Saito, Y.; Pickering, H. W.; Nishina, Y.; Sakurai, T. *Jpn. J. Appl. Phys.* **1993**, *32*, L450.
(26) Wertheim, G. K.; Rowe, J. E.; Buchanan, D. N. E.; Chaban, E. E.; Hebard, A. F.; Kortan, A. R.; Makhija, A. V.; Haddon, R. C. *Science* **1991**, *252*, 1419.
(27) Rinaldi, R.; Cingolani, R.; Jones, K. M.; Baski, A. A.; Morkoc, H.; Carlo, A. D.; Widany, J.; Sala, E. D.; Lugli, P. *Phys. Rev.* **2001**, *B63*, 075311.
(28) Virgili, T.; Lidzey, D. G.; Bradley, D. D. C. *Adv. Mater.* **2000**, *12*, 58.
(29) He, T.; Kanicki, J. *Appl. Phys. Lett.* **2000**, *76*, 661.
(30) Mattoussi, H.; Rubner, M. F.; Zhou, F.; Kumar, J.; Tripathy, S. K.; Chiang, L. Y. *Appl. Phys. Lett.* **2000**, *77*, 1540.
(31) Sariciftci, N. S.; Braun, D.; Zhang, C.; Srdanov, V. I.; Heeger, A. J.; Stucky, G.; Wudl, F. *Appl. Phys. Lett.* **1993**, *62*, 585.
(32) Wan, L. J.; Itaya, K. *Langmuir* **1997**, *13*, 7173.
(33) Wang, D.; Wan, L. J.; Xu, Q. M.; Wang, C.; Bai, C. L. *Surf. Sci.* **2001**, *478*, L320.
(34) Chi, Y.; Bhonsle, J. B.; Canteenwala, T.; Huang, J. P.; Shiea, J.; Chen, B. J.; Chiang, L. Y.*Chem. Lett.* **1998**, *5*, 465.
(35) Li, H.-M.; Xiang, C.-H.; Li, Y.-L.; Xiao, S.-Q.; Fang, H.-J.; Zhu, D.-B. *Synth. Metal.* **2003**, *135*−*136*, 483.
(36) Fan, X. L.; Wang, C.; Yang, D. L.; Wan, L. J.; Bai, C. L. *Chem. Phys. Lett.* **2002**, *361*, 465.
(37) Hou, J. G.; Yang, J. L.; Wang, H. Q.; Li, Q. X.; Zeng, C. G.; Lin, H.; Wang, B.; Chen, D. M.; Zhu, Q. S. *Phys. Rev. Lett.* **1999**, *83*, 3001.
(38) Fasel, R.; Aebi, P.; Agostino, R. G.; Naumović, D.; Osterwalder, J.; Santaniello, A.; Schlapbach, L. *Phys. Rev. Lett.* **1996**, *76*, 4733.